Environ. Sci. Technol. **1999**, *33,* 618−624

Formation of Chloropyromorphite from Galena (PbS) in the Presence of Hydroxyapatite

PENGCHU ZHANG*

Geochemistry Department, MS 0750, Sandia National Laboratories, Albuquerque, New Mexico 87185

JAMES A. RYAN

National Risk Management Research Laboratory, U.S. Environmental Protection Agency, 5995 Center Hill Avenue, Cincinnati, Ohio 45224

Transformation of unstable lead [Pb(II)] forms into sparingly soluble pyromorphite [$Pb_5(PO_4)_3(OH, Cl, F, ...)$] by the addition of phosphate to Pb-contaminated soil has been proposed as a remediation technology to reduce the mobility and bioavailability of Pb. Galena, an insoluble lead sulfide mineral (PbS) frequently found in mining wastes, becomes unstable upon exposure to oxidizing conditions causing it to become a source of liable Pb forms in soils. Thus, a galena ore was reacted with synthetic hydroxyapatite [$Ca_5(PO_4)_3OH$] under various pH conditions to determine the formation rate of pyromorphite and the solubility of galena under the ambient condition. In a 6-day reaction period, the dissolution rate of galena increased with pH due to the oxidation of dissolved sulfide. Hence, formation of chloropyromorphite became apparent in the galena−apatite suspensions with increasing pH. The insignificant effect of mineral P/Pb molar ratio on the formation of chloropyromorphite implied that dissolution/oxidation of galena was the rate-limiting step.

Introduction

In-situ immobilization of soil lead [Pb(II)] by the addition of phosphate minerals has been considered a cost-effective and environmental benign alternative remediation technology for Pb-contaminated soils. This approach transforms the reactive and bioavailable soil Pb species, or labile Pb species, into chemical forms that are stable and have reduced solubility, mobility, and boiavailability under environmental conditions. It has been demonstrated that pyromorphite [$Pb_5(PO_4)_3(OH, Cl, F, ...)$] is one of the most stable Pb forms that can be formed under ordinary soil conditions and that the bioaccessibility of soil Pb can be drastically reduced when unstable soil Pb forms, such as cerrusite ($PbCO_3$), are converted into pyromorphite (*1*). Soluble Pb concentrations in soil solutions have been reduced by the addition of phosphate minerals (*2*−*6*), which has been speculated to be the result of pyromorphite formation. Direct observations of the formation of pyromorphite in aqueous Pb solution, on exchange resin surface, from goethite-adsorbed Pb, anglesite, cerrusite, and Pb-contaminated soil by reaction with hydroxyapatite (*2*, *7*−*11*) have been reported. Additionally, the formation of pyromorphite in contaminated soils and wastes that contained high levels of phosphate has been demonstrated (*8, 12, 13*), and direct evidences of formation of pyromorphite in contaminated soils amended with soluble phosphate and/or hydroxyapatite have been obtained (*6*, *8, 14*).

Although substitution of Pb for Ca in apatite may be possible (*15*), the dominant mechanism of pyromorphite formation in the Pb−P−H_2O system has been reported as precipitation of soluble lead and phosphate (*2, 5, 16*). The precipitation of pyromorphite from the soluble Pb and PO_4 is a rapid process, completed within seconds in solutions that are saturated with respect to pyromorphite (*2*). Thus, the rate of pyromorphite formation in systems containing solid Pb-bearing forms and PO_4 minerals will be determined by the dissolution rate of the solid Pb and/or PO_4 forms. Accordingly, the soluble Pb concentration in an aqueous system containing apatite and Pb-bearing solids will be determined by the dissolution rate of apatite and the overall Pb release rate (desorption, dissociation, and dissolution) of the Pb species. As the forms of soil Pb vary and depending upon the sources of Pb contamination and environmental conditions, knowledge of the reaction behavior of primary Pb forms with phosphate becomes important in assessing the efficiency of Pb immobilization by the addition of phosphate.

Galena, an insoluble lead sulfide mineral (PbS) frequently found in mining wastes and under reducing environments, such as anaerobically digested sludge and anoxic aquatic sediments (*17*−*20*), becomes unstable upon exposure to oxidizing conditions where sulfide is oxidized to a higher oxidation state, eventually to sulfate ion, and Pb ion is released into the solution (*21*). Thus, galena becomes a potential bioavailable Pb species when it is in soils, wastes, and sediments under ambient conditions. Therefore, a series of kinetic experiments were conducted in systems containing hydroxyapatite and galena to determine the effects of dissolution rates of apatite and galena on (i) the rate of formation of pyromorphite and (ii) the soluble Pb level during the reaction. These experiments were conducted in the presence of oxygen, allowing an evaluation of the formation of pyromorphite in aqueous solutions.

Materials and Methods

Minerals. Galena, a lead sulfide ore, obtained from The Doe Run Company was used in this study. Prior to use, the mineral was passed through a 25-μm sieve. The specific surface area of the galena sample was 0.533 $m^2\ g^{-1}$, determined by BET nitrogen absorption surface area analyzer (Gemini III, Micromeritics). The elemental composition of this mineral was 84.7 and 13.5% (w/w %) of Pb and S, respectively. Impurities in the mineral included Zn (0.01%), Fe (0.03%), MgO (0.03%), and Cr (0.05%). The mineral exhibited a characteristic X-ray diffraction (XRD) pattern of galena, and no other minerals were detectable.

A synthetic hydroxyapatite [$Ca_5(PO_4)_3OH$] (obtained from Bio-Rad) was used as the phosphate source. The specific surface area of the mineral was 67.3 $m^2\ g^{-1}$, determined by a BET nitrogen absorption. The molar ratio of P/Ca of the apatite was 1.62, which is close to the ideal ratio of 1.67.

Dissolution of Galena and Hydroxyapatite. Dissolution of galena was conducted in a brown glass bottle containing 1.0 L of 0.10 M $NaNO_3$ and 0.001 M NaCl solution. Prior to the addition of 0.120 g of galena (5.0×10^{-1} mmol), the solution was adjusted with 0.1 N HNO_3 to a pH of 2, 3, 4, 5, 6, or 7. The pH was maintained with an automatic titrator for 30 min after the addition of galena. The bottles containing

* To whom correspondence should be addressed. Telephone: (505)844-2669; fax: (505)844-7354; e-mail: pzhang@sandia.gov.

10.1021/es980314a CCC: $18.00
Published on Web 01/05/1999

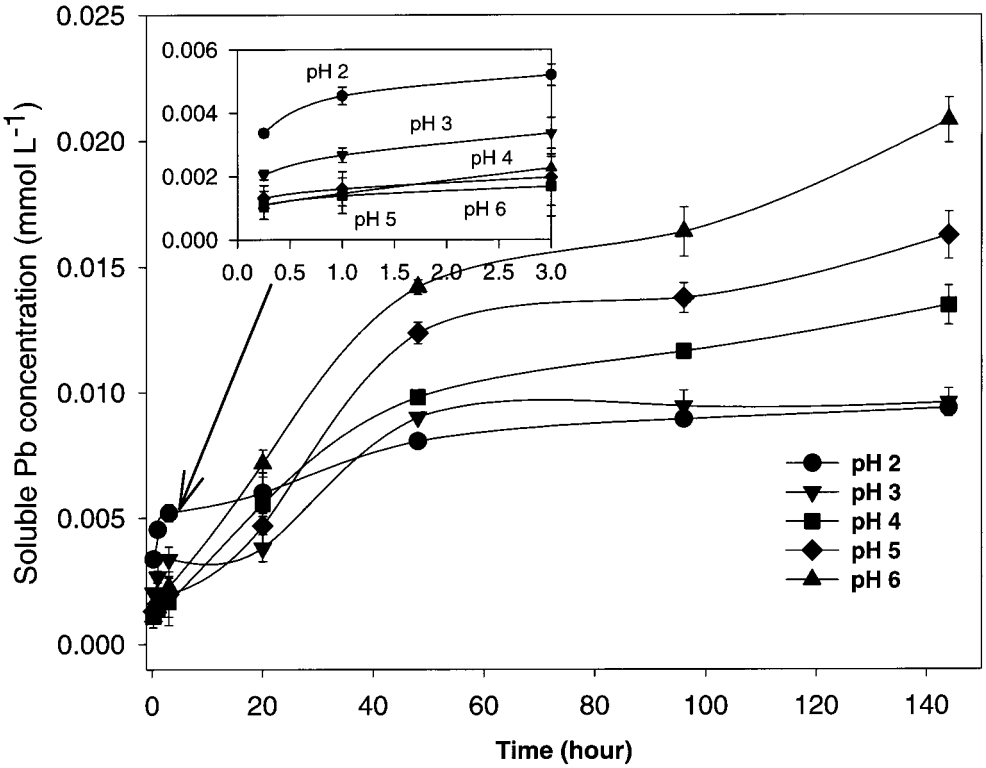

FIGURE 1. Effect of pH on galena dissolution. Soluble Pb is used to present the dissolution of galena. The insert is the dissolution in the initial 180 min.

the suspensions were then capped and rotated on a parallel rotator. The suspension pH was monitored and adjusted as needed. Suspension samples were periodically taken with a syringe and filtered with a 0.2-μm membrane, and the filtrates were analyzed for soluble Pb and S on an inductively coupled plasma spectrophotometer (ICP). The dissolution of galena was determined by measuring the soluble Pb and S concentrations as a function of time. Determination of hydroxyapatite dissolution rates has been described previously (*11*).

Reactions between Galena and Hydroxyapatite. The reactions between galena and hydroxyapatite were carried out at three molar ratios of P/Pb (3/5, 6/5, and 12/5) established by mixing 0.12 g (5.0×10^{-1} mmol) of galena with 0.05 g (1×10^{-1} mmol), 0.10 g (2×10^{-1} mmol), and 0.20 g (4×10^{-1} mmol) of hydroxyapatite, respectively. The amount of phosphate contained in the added hydroxyapatite was one, two, and four times that needed to stoichiometrically react with the Pb contained in 0.12 g of galena to form pyromorphite [$Pb_5(PO_4)_3Cl$]. For each of these three P/Pb ratio experiments, the reaction was conducted at a pH of 2, 3, 4, 5, and 6. After adding the galena−apatite mixture into 1.0 L of 0.10 M $NaNO_3$ and 0.001 M NaCl solution, the suspension was stirred for 2 h while the pH was maintained with an automatic titrator. The suspension was then placed into a brown bottle, capped, and rotated on a parallel rotator. The suspension pH was monitored and adjusted as needed. The suspensions were periodically sampled with decreasing frequency during the 6-day reaction period. Sampled suspensions were filtered through a 0.2-μm membrane, and the filtrates were analyzed for PO_4, Ca, Pb. and S using ICP. At the end of the experiment, the solids were collected, and their mineral composition and surface chemical composition and morphology were determined using XRD and a scanning electronic microscope equipped with energy-dispersive X-ray spectroscopy (SEM/EDX).

Analytical Procedures. An inductively coupled plasma spectrophotometer (Trace 61E, Thermal Jarrell Ash) was used to quantify soluble Pb, PO_4, Ca, and S. The detection limit for these four elements was 2 μg L^{-1}. The Water Supply Performance Evaluation Study solution (WS033) by the U.S. EPA was used to calibrate and verify the analytical standard solutions used for ICP analysis. Experimental blanks, standards, and spiked samples were used for analytical quality control. Solution and suspension pH were measured by a glass pH electrode that was connected to the Mettler titrator. With this setup, the variation of pH could be maintained within 0.01 pH unit.

The solid samples were examined with an X-ray diffractometer (Scintag, XDS 2000; Cu-Kα radiation at 35 kV filament current of 30 mA) and a step-scanning rate of 0.04° 2θ/s was employed. A scanning electron microscope coupled with energy-dispersive X-ray spectroscope (SEM/EDX, JEOL, JSM 5300) was used to obtain the solid images and surface elemental composition.

Results

Dissolution of Galena and Hydroxyapatite. *Dissolution of Galena.* As measured by soluble Pb concentration, dissolution of galena increased as pH decreased during the initial 180-min reaction time (Figure 1, insert). Soluble S concentrations (not shown) were similar to soluble Pb, thus dissolution of galena was stoichiometric.

In contrast, after longer reaction times, the dissolution rate of galena was positively related to suspension pH (Figure 1). After 144-h reaction time, the soluble Pb was 8.0×10^{-2} mmol L^{-1} at pH 2 and pH 3 and increased to 1.2, 1.6, and 2.0×10^{-1} mmol L^{-1} at pH 4, 5, and 6, respectively (Figure 1).

Dissolution of Hydroxyapatite. The dissolution rate of hydroxyapatite is inversely related to pH, and the dissolution reached a steady state in approximately 60 min. The detailed discussion of apatite dissolution can be found elsewhere (*11*).

Reactions of Galena and Hydroxyapatite. The formation of pyromorphite is the dominant process in the systems containing soluble Pb and phosphate (*5, 22, 23*) or solid Pb-bearing forms such as cerrusite and anglesite on reaction with apatite (*12, 14*). If chloride ions, Cl^-, are present, the reaction product will be chloropyromorphite [$Pb_5(PO_4)_3Cl$], the least soluble form in the pyromorphite mineral group. Accordingly, the removal of soluble Pb and PO_4 from solution in these galena−apatite suspensions was attributed to precipitation of chloropyromorphite. This assumption is ultimately verified with XRD and EDX analysis. In suspensions involving dissolution of apatite and galena, there were no processes such as adsorption and precipitation to remove soluble Ca and S from solutions. Thus, soluble Ca and S concentrations were used to determine the quantities of apatite and galena dissolved. Considering the oxidation of dissolved sulfide, calcium sulfate ($CaSO_4 \cdot 2H_2O$, gypsum) was the most probable mineral formed from Ca^{2+} and SO_4^{2-}; however, gypsum has a relatively high solubility product (4.5×10^{-5}) that apparently, as demonstrated later, precluded precipitation in these suspensions.

Soluble Species. Soluble S concentrations as a function of reaction time for the three P/Pb ratios of 3/5, 6/5, and 12/5 are presented in Figure 2, panels a−c, respectively. At pH 2 and pH 3, the soluble S levels were equal at 1.2 (± 0.2) $\times 10^{-2}$ mmol L^{-1} for the three P/Pb ratios after 144-h reaction time (Figure 2a−c). As pH increased, soluble S concentrations increased, and the average concentration of S in the three P/Pb ratio solutions were 2.5 (± 0.5), 3.0 (± 0.6), and 4.0 (± 0.5) $\times 10^{-2}$ mmol L^{-1} at pH 4, 5, and 6, respectively (Figure 2a−c). This increase was more apparent at the longer reaction times, (Figure 2a−c). Thus, there was no significant effect of the P/Pb ratio on galena dissolution. However, there was a greater S concentration in the systems that contain apatite, indicating a greater dissolution of galena in the present of apatite.

At low pH values of 2 and 3, the soluble Pb concentrations, $1.0-1.4 \times 10^{-3}$ mmol L^{-1} (Figure 3), were approximately equalvent to that of soluble S, 1.2 (± 0.2) $\times 10^{-3}$ mmol L^{-1} (Figure 2a−c) when the reactions reached an apparent steady state, about 48 h. This stoichiometric composition with respect to galena indicates limited removal of S or Pb from the solutions at pH 2 and pH 3. Thus, the formation of lead phosphate(s) or chloropyromorphite at these pH values was limited. At pH 4, the soluble Pb concentrations were 2.0, 1.0, and 0.2 $\times 10^{-3}$ mmol L^{-1} in the suspensions with P/Pb ratios of 3/5, 6/5, and 12/5, respectively, after 48-h reaction time (Figure 3a−c). At pH 5 and pH 6, the Pb concentrations were below 2 μg L^{-1} (1×10^{-5} mmol L^{-1}), which was the analytical detection limit, in all of the suspensions after the first 60-min reaction (Figure 3a−c). These soluble Pb levels were 1−5 orders of magnitude lower than that of soluble S and, thus, lacked stoichiometry with respect to dissolution of galena. The disappearance of dissolved Pb can be attributed to the formation of chloropyromorphite. The dissolved Pb from galena in these suspensions was readily precipitated as chloropyromorphite because of the high availability of soluble PO_4 from the dissolution of apatite. At pH 5 and pH 6, the soluble PO_4 levels ranged from $2 \times 10^{-1}-10^{0}$ mmol L^{-1} (Figure 4), and the soluble Pb concentrations were at levels of 10^{-6} and 10^{-7} mmol L^{-1} (Figure 3), which agreed with the results calculated from the solubility of chloropyromorphite at these pH values (*16*). Thus, the formation of chloropyromorphite can be assumed to have occurred.

The mass balance calculation from the soluble S or Pb concentration indicated that only a small portion of the added galena was involved in the reactions during the 144-h reaction. At pH 2 and pH 3, 2−3% of the added galena was dissolved. At pH 4, 5, and 6, 5 (± 1), 6 (± 1.2), and 8 (± 1)%, respectively, of the added galena was dissolved.

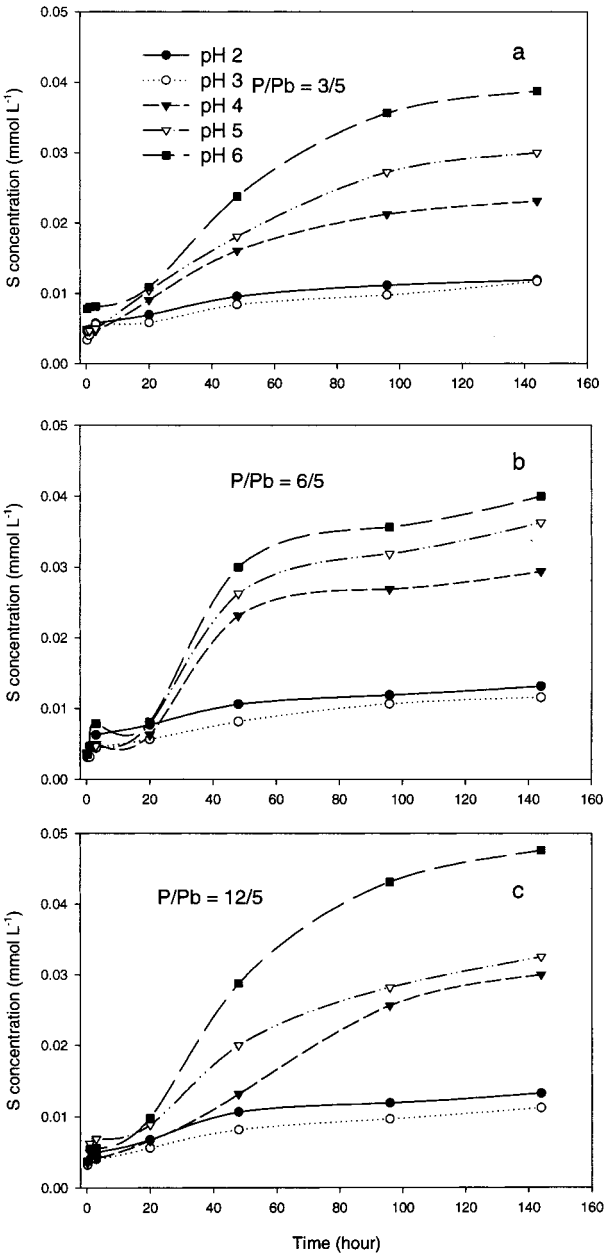

FIGURE 2. Soluble sulfur concentrations in the galena−hydroxyapatite suspensions under various pH values and P/Pb molar ratios.

At the low pHs (2 and 3), the added hydroxyapatite was completely dissolved within 120 min (Figure 4). Above pH 3, the amount of apatite dissolution decreased with increasing pH as indicated by the soluble PO_4 (Figure 4) and Ca (not shown), resulting in a soluble PO_4 in the range of $1.5-6 \times 10^{-1}$ mmol L^{-1} in the P/Pb ratios of 3/5 and 6/5 and $0.5-1.5 \times 10^{-3}$ mol L^{-1} in the P/Pb ratio of 12/5 (Figure 4a−c). This greater dissolution of apatite as compared to galena assured the availability of soluble PO_4; thus, it was not limiting the precipitation of the soluble Pb to form chloropyromorphite.

Mineralogical Analysis. A series of SEM images were taken of the solids collected after 144-h reaction time. As the solids from the three P/Pb ratio experiments were similar, the images from P/Pb = 6/5 were presented as an example (Figure 5). There was no new phase formed in the solid collected at pH 2; the cubic-shaped galena was the only mineral in the suspension (Figure 5a). At pH 3, there were a few tiny, needle-shaped particles observed in addition to the dominant galena particles (Figure 5b). The chemical composition analysis of this needle-shaped solid surface, as illustrated by the EDX

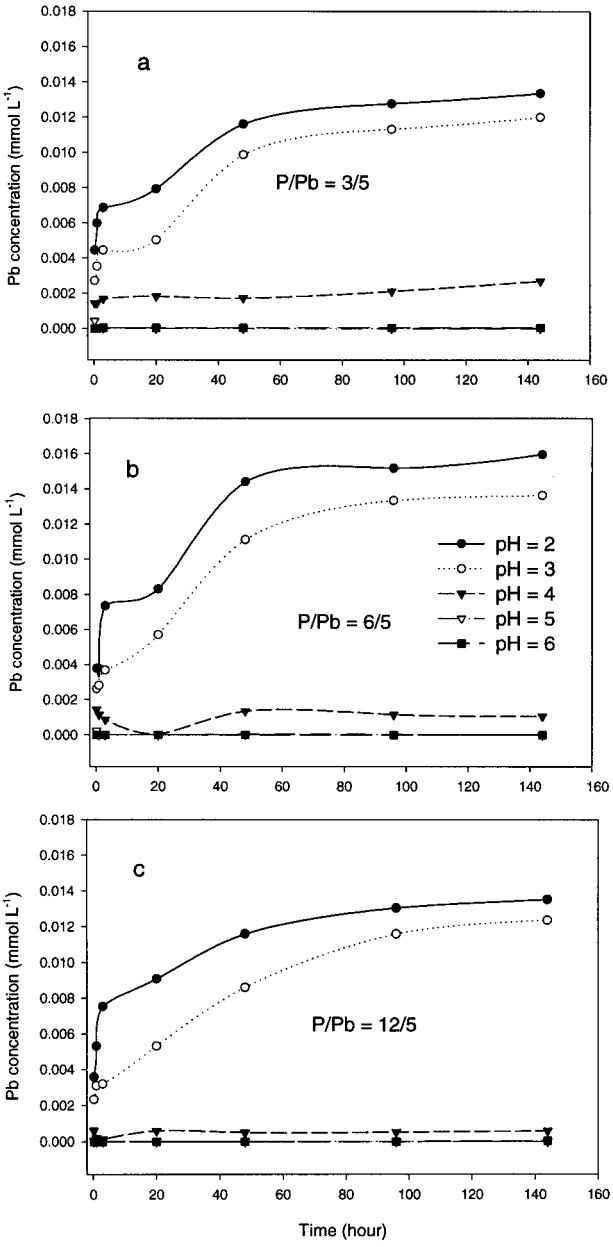

FIGURE 3. Soluble lead concentrations in the galena–hydroxyapatite suspensions under various pH values and P/Pb molar ratios.

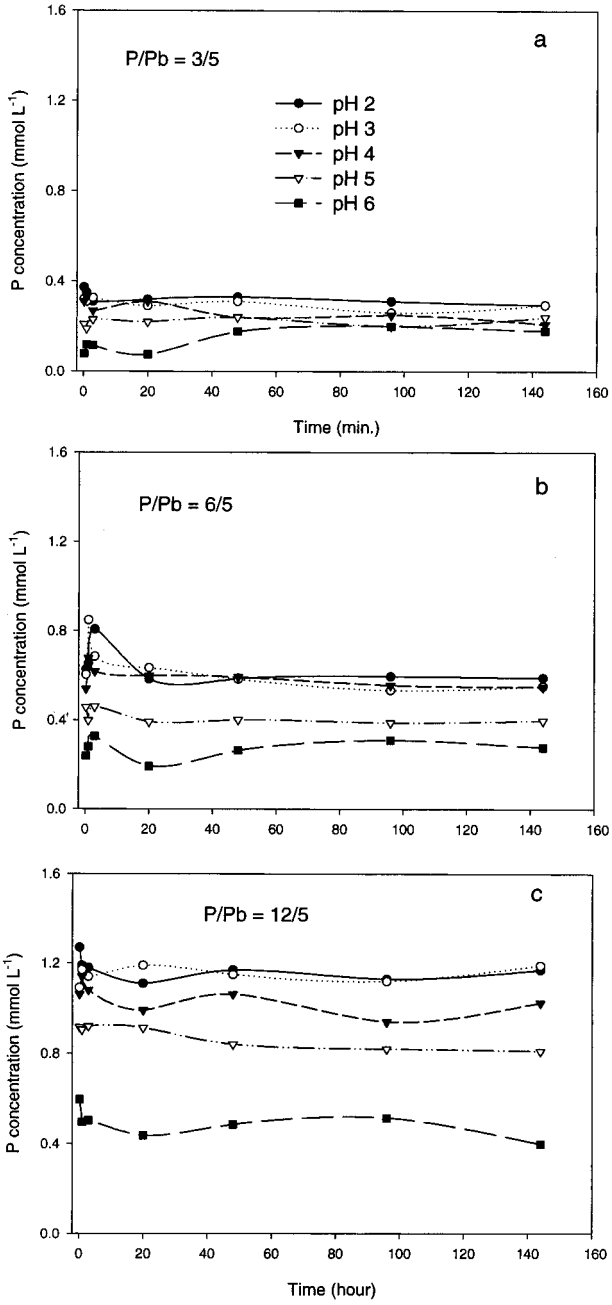

FIGURE 4. Soluble phosphate concentrations in the galena–hydroxyapatite suspensions under various pH values and P/Pb molar ratios.

spectrum of Figure 6a, indicates an elemental ratio of Pb, P, and Cl similar to a synthetic chloropyromorphite (Figure 6c). The needle-shaped particles became more apparent in the solids collected at pH 4 (Figure 5c). At pH 5 and pH 6, the newly precipitated particles developed on the surface of apatite, which was not completely dissolved at these pH values (Figure 5d,e). The EDX spectrum includes Ca in addition to Pb, P, and Cl (Figure 6b). This observation implies that the spectra reflect the elements consisting of chloropyromorphite [$Pb_5(PO_4)_3Cl$] and hydroxyapatite [$Ca_5(PO_4)_3OH$]. Calcium was not found in spectra of solids at pH 3 (Figure 6a) and pH 4 (not shown) because the newly precipitated crystals were formed in solution rather than on the apatite surface. This observation is consistent with the results from solution analysis in which complete dissolution of the added apatite was achieved at pH 3 and pH 4. Therefore, the crystallization of chloropyromorphite occurred in the solution. In contrast, incomplete dissolution of apatite at pH 5 and pH 6 provided a surface for chloropyromorphite precipitation.

As indicated by the results from the solution analysis, only a small portion of added galena was dissolved; therefore, the amount of dissolved Pb involved in precipitation with phosphate to form chloropyromorphite was limited. This low content of chloropyromorphite in the mixture of galena and apatite was insufficient to generate a visible XRD pattern for chloropyromorphite. Therefore, powder X-ray diffraction analysis did not demonstrate the characteristic patterns for chloropyromorphite in the solids collected at pH 3, 4, and 5. However, the characteristic chloropyromorphite peaks were obtained in the solid collected at pH 6 for P/Pb = 12/5 (Figure 7a). In this treatment, about 9% of the added galena-Pb was converted to chloropyromorphite-Pb. As shown in Figure 7a, one of the chloropyromorphite peaks at the 30.08° 2θ is overlapped by a galena peak at 30.19° 2θ. However, another characteristic peak of chloropyromorphite at 30.94° 2θ was apparent (Figure 7a). To confirm the formation of

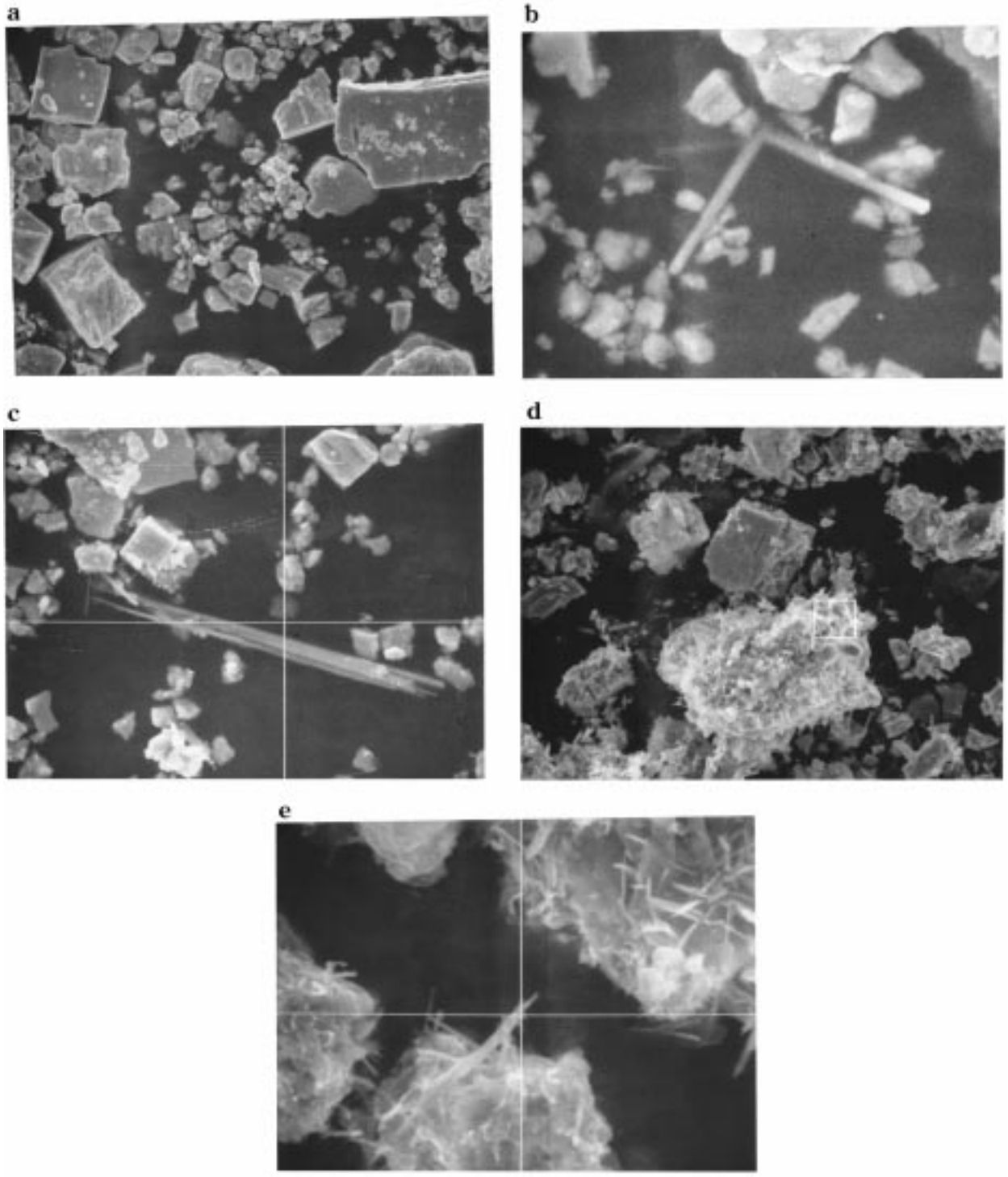

FIGURE 5. SEM images for the solids collected from galena−hydroxyapatite suspensions after 144-h reaction time under various pH conditions: (a) pH 2, (b) pH 3, (c) pH 4, (d) pH 5, and (e) pH 6.

chloropyromorphite in the galena−apatite suspension, the XRD patterns for the galena used in this study and a synthetic chloropyromorphite were also presented in Figure 7b,c.

Discussion

The quantities of galena dissolved in the first 180-min reaction obtained in this study were in general agreement with that reported by others elsewhere (*21*). Apparently, surface protonation, adsorption of H^+ on the mineral surface is the first step for most mineral dissolution processes and was the driving force in the galena dissolution. At low pH, the high proton concentration enhanced the surface protonation and thus increased dissolution rate:

$$PbS(s) + 2H^+ = PbSH_2^{2+}(s) \rightarrow Pb^{2+} + H_2S \qquad (1)$$

The pH_{zpc} (the pH at zero point of charge of a surface) of galena is between 2 and 4, depending upon the galena sources (*21*). At pH < 4, the surface is positively charged [$PbSH_2^{2+}(s)$] because of the adsorption of protons, and a higher dissolution of galena can be expected. This was confirmed by the results obtained in the initial 180-min reaction (Figure 1). Between pH 4 and pH 8, the net charge of the surface is either neutral

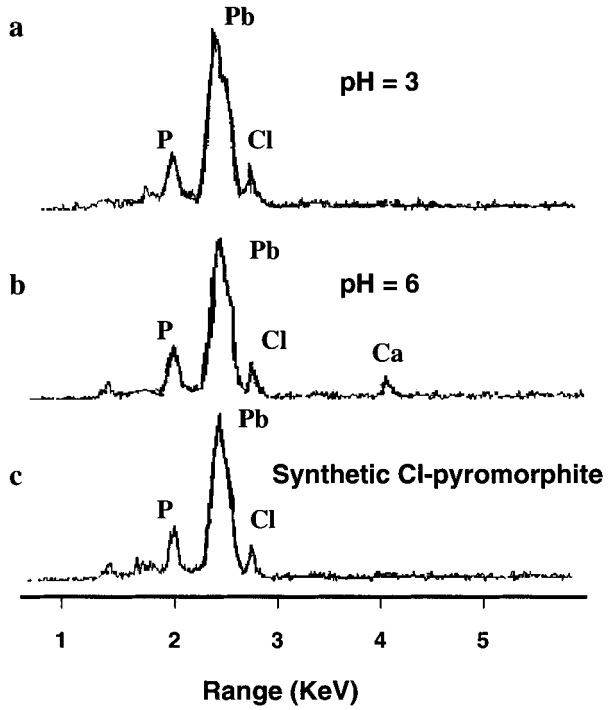

FIGURE 6. EDX spectra for the new solid phase in the galena–hydroxyapatite suspension after 144-h reaction time at pH 3 (a), pH 6 (b), and a synthetic chloropyromorphite (c).

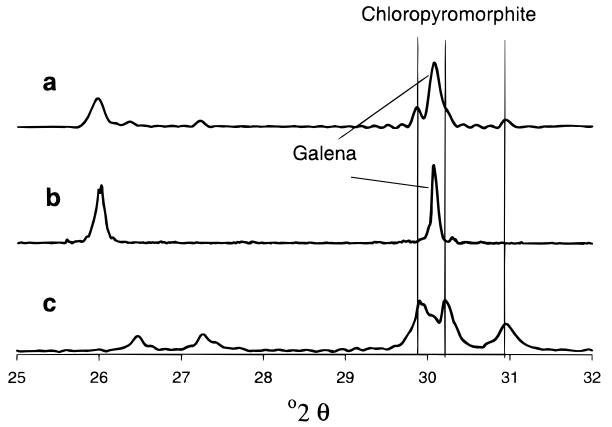

FIGURE 7. XRD pattern for the solid collected in the galena–hydroxyapatite suspension reacting for 144 h at pH 6 (a), the galena mineral used in this study (b), and the synthetic chloropyromorphite (c).

or negative, thus dissolution of galena can be limited by the low surface protonation (*21*).

Soluble sulfide is not stable and will be transformed into the species with higher oxidation state such as S^0, S_2O_3, SO_3, and SO_4 in the presence of oxygen (*21*, *24*, *25*). Dissolution of galena was carried out under aerobic condition. Therefore, oxidation of dissolved sulfide would lower the activity of soluble sulfides (H_2S and HS^-) and decrease the degree of saturation with respect to galena, resulting in increasing dissolution. The oxidation from sulfide to SO_4, the final oxidation product, was demonstrated to be completed within 6 h (*21*). However, the effect of pH on sulfide oxidation under constant oxygen partial pressure condition suggested an increase in oxidation rate constants with increasing pH, especially in the pH range of 4–8 (*25*). The rate of oxidation of soluble sulfide to element sulfur was extremely slow when the pH was lower than 6 but sharply increased from pH 6 to pH 7 (*24*). The measured oxidation rate constant (log *k*) increased from 1.85 at pH 1.95 to 2.33 at pH 6.17, with the greater increase occurring from pH 4 to pH 6 (*25*). This appears to agree with the results from galena dissolution in this study in which the dissolution rates at pH 2 and pH 3 were approximately equivalent and the rate increased significantly from pH 4 to pH 6 within the 144-h reaction time (Figure 1). The higher oxidation of dissolved sulfide, observed at higher pH, removed soluble sulfide making the solution undersaturated with respect to galena and resulted in an increase in galena dissolution (Figure 1). The estimated half time ($t_{1/2}$) of oxidation ranged from 20 to 50 h (*25*). The difference in galena dissolution became apparent in a relatively long reaction time (Figure 1), which is consistent with the results obtained in a later study (*25*). The higher dissolution of galena at higher pH values may imply that the higher transformation of Pb from galena to pyromorphite can be observed.

In the suspensions containing galena and hydroxyapatite, chloropyromorphite cannot be formed directly as the overall reaction:

$$Ca_5(PO_4)_3OH(s) + 5PbS(s) + Cl^- + H^+ = Pb_5(PO_4)_3Cl(s) + 5S^{2-} + 5Ca^{2+} + H_2O \quad (2)$$

cannot be carried out spontaneously, ($\Delta G_f = +345.7$ kJ mol^{-1}). In the presence of oxygen, the dissolved sulfide is oxidized, and the sulfur species with higher oxidation states such as S^0, S_2O_3, and SO_4 will be formed. Considering sulfide oxidation, the possible reactions depending upon the oxidation products in the galena and apatite suspensions can be expressed as

$$Ca_5(PO_4)_3OH(s) + 5PbS(s) + Cl^- + 11H^+ + 5/2O_2 = Pb_5(PO_4)_3Cl(s) + 5S^0 + 5Ca^{2+} + 6H_2O \quad (3)$$

$$\Delta G_f = -960.0 \text{ kJ mol}^{-1}$$

and/or

$$Ca_5(PO_4)_3OH(s) + 5PbS(s) + Cl^- + H^+ + 10O_2 = Pb_5(PO_4)_3Cl(s) + 5SO_4^{2-} + 5Ca^{2+} + H_2O \quad (4)$$

$$\Delta G_f = -2426.6 \text{ kJ mol}^{-1}$$

Reactions 3 and 4 will take place spontaneously, and the formation of chloropyromorphite can be expected under aerobic conditions as used in this study. Although various oxidation products can be formed, the sulfur–oxygen anions such as S_2O_3, SO_3, and SO_4 are the more likely oxidation products of dissolved sulfide (*21*, *25*).

At the low pH values, e.g., 2 and 3, the oxidation rate of dissolved sulfide was slow, thus the amount of dissolved galena, about 1×10^{-2} mmol (Figure 2), was equal for the solutions without and with apatite addition (Figure 1 vs Figure 2). The soluble Pb concentrations (Figure 3) were approximately equivalent to the soluble S (Figure 2) at pH 2 and pH 3, indicating a lack of removal of soluble Pb from the solution. Formation of chloropyromorphite at these pH values was limited. In contrast, the amount of galena dissolution in the apatite added suspensions was nearly doubled at pH 4 and above (Figure 2) as compared to that of galena alone (Figure 1). This implies that the formation of chloropyromorphite in the suspension depleted the soluble Pb from the solutions (Figure 3) and enhanced dissolution of galena and oxidation of dissolved sulfide. The SEM analysis (Figure 5) in which chloropyromorphite was not found in pH 2 but became more apparent with increasing pH confirms this conclusion. Accordingly, both dissolution of galena and

formation of chloropyromorphite were determined by the rate of dissolved sulfide oxidation.

At pH 4 and above, the measured soluble Pb concentrations in the three P/Pb ratio suspensions were in the range determined by the solubility of chloropyromorphite; similar results were determined by the geochemical model simulation, EQ3 (*26*). This further confirmed the formation of chloropyromorphite in the suspensions and also implied the oxidation occurrence in the suspension. If the dissolved sulfide was not oxidized, the solutions would be supersaturated with respect to galena as indicated by the soluble S concentration in Figure 2, and further dissolution of galena would be prohibited. Assuming the predominant final oxidation product of the sulfide was SO_4 (*21*), lead sulfate ($PbSO_4$ or anglesite) could remove the soluble Pb from solution. However, at pH 4 the solubility of chloropyromorphite was several orders of magnitude lower than that of anglesite (*27*), thus solutions were saturated with respect to chloropyromorphite and the formation of anglesite was not possible. This was further confirmed by the XRD analysis (Figure 7) and the simulated species distribution by EQ 3. These results suggested that, in an aerobic aqueous suspension of galena, the formation of chloropyromorphite was determined by the oxidation rate of sulfide and that the soluble Pb concentration was determined by the solubility of the newly formed chloropyromorphite in the presence of apatite.

Literature Cited

(1) Laperche, V.; Logan, T. J.; Gaddam, P.; Traina, S. J. *Environ. Sci. Technol.* **1997**, *31*, 2745.
(2) Ma, Q. Y.; Traina, S. J.; Logan, T. J.; Ryan, J. A. *Environ. Sci. Technol.* **1993**, *27*, 1803.
(3) Ma, Q. Y.; Logan, T. J.; Traina, S. J. *Environ. Sci. Technol.* **1995**, *29*, 1118.
(4) Ma, L. Q. *J. Environ. Qual.* **1996**, *25*, 1420.
(5) Xu, Y.; Schwartz, F. W. *J Contam. Hydrol.* **1994**, *15*, 187.
(6) Zhang, P.-C.; Ryan, J. A. *Soil Science Society of America Annual Meeting*; ASA SSSA: St. Louis, MO, 1995; p 41.
(7) Ruby, M. V.; Davis, A.; Nicholson, A. *Environ. Sci. Technol.* **1994**, *28*, 646.
(8) Zhang, P.; Ryan, J. A.; Bryndzia, L. T. *Environ. Sci. Technol.* **1997**, *31*, 2673.
(9) Zhang, P.; Ryan, J. A. *Environ. Sci. Technol.* **1998**, *32*, 3318.
(10) Zhang, P.; Ryan, J. A. *Environ. Sci. Technol.* In press.
(11) Zhang, P.-C.; Ryan, J. A.; Yang, J. *Environ. Sci. Technol.* **1998**, *32*, 2763.
(12) Cotter-Howells, J.; Cahmpness, P. E.; Charnock, J. M.; Pattrick, R. A. D. *Eur. J. Soil Sci.* **1994**, *45*, 393.
(13) Cotter-Howells, J. *Environ. Pollut.* **1995**, *90*, 1.
(14) Laperche, V.; Traina, S. J.; Gaddam, P.; Logan, T. J. *Environ. Sci. Technol.* **1996**, *30*, 3321.
(15) Cotter-Howells, J.; Caporn, S. *App. Geochem.* **1996**, *11*, 335.
(16) Nriagu, J. O. *Inorg. Chem.* **1972**, *11*, 2499.
(17) Morel, F. M. M.; Westall, J. C.; O'Melia, C. R.; Morgan, J. J. *Environ. Sci. Technol.* **1975**, *9*, 756.
(18) Rohatgi, N.; Chen, K. Y. *Water Pollut. Control Fed.* **1975**, *47*, 2298.
(19) Rohatgi, N.; Chen, K. Y. *J. Environ. Eng. Div. ASCE* **1976**, *102*, 675.
(20) Ruby, M. V.; Davis, A.; Kempton, J. H.; Drxler, J. W.; Bergstrom, P. *Environ. Sci. Technol.* **1992**, *26*, 1242.
(21) Hsieh, Y. H.; Huang, C. P. *J. Colloid Interface Sci.* **1989**, *131*, 537.
(22) Nriagu, J. O. *Geochim. Cosmochim. Acta.* **1974**, *38*, 887.
(23) Nriagu, J. O.; Moore, P. B. *Phosphate Minerals*; Springer-Verlag: New York, 1983.
(24) Chen, K. Y.; Morris, J. C. *Environ. Sci. Technol.* **1972**, *6*, 529.
(25) Millero, F. J.; Hubinger, S.; Fernandez, M.; Garnett, S. *Environ. Sci. Technol.* **1987**, *21*, 439.
(26) Wolery, T. J. *EQ3/6, A software package for geochemical modeling of aqeous systems*; Lawrence Livermore National Laboratory: Livermore, CA, 1992.
(27) Lindsay, W. L. *Chemical equilibria in soils*; Wiley & Sons: New York, 1979.

Received for review March 30, 1998. Revised manuscript received November 4, 1998. Accepted November 4, 1998.

ES980314A